International Journal of Materials Science and Applications
2019; 8(1): 12-20
http://www.sciencepublishinggroup.com/j/ijmsa
doi: 10.11648/j.ijmsa.20190801.12
ISSN: 2327-2635 (Print); ISSN: 2327-2643 (Online)

Dielectric and Ferroelectric Properties of Ho_2O_3 Doped Barium Strontium Titanate Ceramics

Mengyuan Zhang, Congyu Li, Fangxu Chen, Long Chen, Jianhua Liu, Tianyu Chen, Chen Zhang*

Department of Materials Science and Engineering, Jiangsu University of Science and Technology, Zhenjiang, China

Email address:
czhang1981@hotmail.com (Chen Zhang)

*Corresponding author

To cite this article:
Mengyuan Zhang, Congyu Li, Fangxu Chen, Long Chen, Jianhua Liu, Tianyu Chen, Chen Zhang. Dielectric and Ferroelectric Properties of Ho_2O_3 Doped Barium Strontium Titanate Ceramics. *International Journal of Materials Science and Applications*. Vol. 8, No. 1, 2019, pp. 12-20. doi: 10.11648/j.ijmsa.20190801.12

Received: July 16, 2018; **Accepted**: August 2, 2018; **Published**: June 26, 2019

Abstract: The crystalline structure, surface morphology, dielectric and ferroelectric properties of 0~10wt% Ho_2O_3 doped $(Ba_{0.75}Sr_{0.25})$ TiO_3 ceramics prepared by conventional solid state method were studied using X-ray diffractometer, scanning electron microscopy, LCR measuring system and ferroelectric property test systems aiming for ceramic capacitor applications. It is found that proper amount of Ho_2O_3 can refine grains of the system. With the increase of Ho_2O_3 doping content, the average grain size of $(Ba_{0.75}Sr_{0.25})$ TiO_3 ceramics decreases. When Ho_2O_3>8 wt%, $(Ba_{0.75}Sr_{0.25})$ TiO_3 based ceramic samples are multi-phase compounds with typical perovskite structure accompanied by the appearance of cylindrical grains. The Ho^{3+} ions substitute the host A sites and B sites of $(Ba_{0.75}Sr_{0.25})$ TiO_3 perovskite lattice, resulting in the lattice distortion of the system and the change of the relative dielectric constant and dielectric loss at room temperature. With the increase of Ho_2O_3 doping content, the relative dielectric constant at room temperature of the system increases first and then decreases. The maximum of relative dielectric constant at room temperature can be found in the 1 wt% Ho_2O_3 doped $(Ba_{0.75}Sr_{0.25})$ TiO_3 ceramics. When Ho_2O_3＞1 wt%, the maximum of relative dielectric constant ε_{rmax} decreases and the temperature corresponding to the maximum of relative dielectric constant T_m shifts toward lower temperature with the increase of Ho_2O_3 doping content. The $(Ba_{0.75}Sr_{0.25})$ TiO_3 ceramics with high Ho_2O_3 content show relaxor-like behavior which is characterized by the typical diffuse phase transition and frequency dispersion of dielectric constant. However, the $(Ba_{0.75}Sr_{0.25})$ TiO_3 ceramics with low Ho_2O_3 content do not exhibit permittivity frequency dispersion. According to the *P-E* hysteresis loops of Ho_2O_3 doped $(Ba_{0.75}Sr_{0.25})$ TiO_3 ceramics, the ferroelectricity was increased and then decreased with the increase of Ho_2O_3 doping content. With the increase of Ho_2O_3 doping content, the *P-E* relationships turn out to be straight lines, implying the paraelectric phase for $(Ba_{0.75}Sr_{0.25})$ TiO_3 ceramics with high Ho_2O_3 content.

Keywords: Barium Strontium Titanate, Perovskite, Relaxor Characteristic, Ferroelectric Properties

1. Introduction

Barium strontium titanate ($(Ba_{1-x}Sr_x)$ TiO_3, BST), as an infinite solid solution of $BaTiO_3$ and $SrTiO_3$, maintains perovskite structure (ABO_3) similar to $BaTiO_3$, and has outstanding properties such as high dielectric constant, low dielectric loss and excellent ferroelectric properties [1-2]. In addition, its Curie temperature can be adjusted over a wide range of temperature by changing Ba/Sr ratio, making the BST systems become one of the basic ceramic materials for ceramic capacitors [3].

As an important component of electronic products, ceramic capacitors require superior and more stable performance in smaller sizes. In order to meet the needs in different applications, people add metal oxides or their derivatives to BST systems to improve their comprehensive properties. The rare earth metal oxides play important roles in the property modification for dielectric materials, which has aroused great interest of many researchers [4-9]. D. C. Sinclair et al. studied the rare earth metal ions RE^{3+} doped barium titanate ceramics, and proposed that when the RE^{3+} ions enter the A site of the perovskite lattice, charge imbalance is created which must be compensated by either cation vacancies on the A or B site (ionic compensation), or by electrons (electronic

compensation) [10-11]. Three point defect reactions can be identified:

$$2RE_2O_3 + 3TiO_2 \rightarrow 4RE^{\bullet}_{Ba} + 3Ti_{Ti} + 12O_o + V^{''''}_{Ti} \quad (1)$$

$$RE_2O_3 + 3TiO_2 \rightarrow 2RE^{\bullet}_{Ba} + 3Ti_{Ti} + 9O_o + V^{''}_{Ba} \quad (2)$$

$$2RE_2O_3 + 4TiO_2 \rightarrow 4RE^{\bullet}_{Ba} + 4Ti_{Ti} + 12O_o + O_2\uparrow + 4e^{'} \quad (3)$$

When the RE^{3+} ions enter the B site of the perovskite lattice, charge imbalance is created which must be compensated by the oxygen vacancies [10]. The point defect reaction can be seen as follows:

$$2BaO + RE_2O_3 \rightarrow 2Ba_{Ba} + 2RE^{\bullet}_{Ti} + 5O_O + V^{\bullet\bullet}_O \quad (4)$$

In general, the large size RE^{3+} ions tend to occupy the A site; The small size RE^{3+} ions tend to occupy the B site; The middle size RE^{3+} ions have the amphoteric behavior occupying both A and B site [12]. Y. Li et al. studied on the dielectric properties of Sm_2O_3 doped $Ba_{0.68}Sr_{0.32}TiO_3$ ceramics, and proposed that the substitution preference of Sm^{3+} in the lattice also depends on Sm_2O_3 doping content [13]. C. Zhao et al. prepared Y_2O_3 and Dy_2O_3 doped $Ba_{0.7}Sr_{0.3}TiO_3$ ceramics with comprehensive properties (ε_r=3.66×10^3, $tan\delta$=9.3×10^{-3}, $\Delta\varepsilon_r/\varepsilon_r$=14.1%) [14]. In addition, some researchers studied the effect of grain size on dielectric and ferroelectric properties of $Ba_{0.80}Sr_{0.20}TiO_3$ ceramics [15-16].

In our present work, 0~10 wt% Ho_2O_3 doped $(Ba_{0.75}Sr_{0.25})TiO_3$ ceramics were prepared by solid state reaction method. The effects of Ho_2O_3 doping content on crystalline structure, surface morphology, dielectric and ferroelectric properties of the system were investigated. The substitution characteristics of Ho^{3+} ions in $(Ba_{0.75}Sr_{0.25})TiO_3$ perovskite lattice will be determined and the interrelationship between the macroscopic dielectric constant, dielectric loss, temperature-dependent properties and microscopic defect behavior will also be established.

2. Experimental

2.1. Sample Preparation

In this paper, high purity $BaCO_3$ (>99.0%), $SrCO_3$ (>99.0%) and TiO_2 (>98.0%) powders used as starting raw materials were proportionally weighed according to the formula $(Ba_{0.75}Sr_{0.25})TiO_3$ and ball-milled for 24 h. After drying, the obtained powders were calcined at 1080°C for 2 h to form main crystalline phase. The calcined powders were mixed with 0.2 wt% MgO (≥98.5%)、0.2 wt% ZnO (≥99.0%) and 0~10 wt% Ho_2O_3(>99.0%), reground for 24 h, dried and added with 5 wt% polyvinyl alcohol (PVA) as a binder for granulation. The mixtures were sieved through 40-mesh screen and then pressed into pellets 10mm in diameter and 2~3 mm in thickness. Sintering was conducted in air at 1400°C for 2 h, and the sintering regime was illustrated on Figure 1. For dielectric properties measurement, both the flat surfaces of the sintered samples were coated with BQ-5311 silver paste after ultrasonic bath cleaning and then fired at 800°C for 10 min.

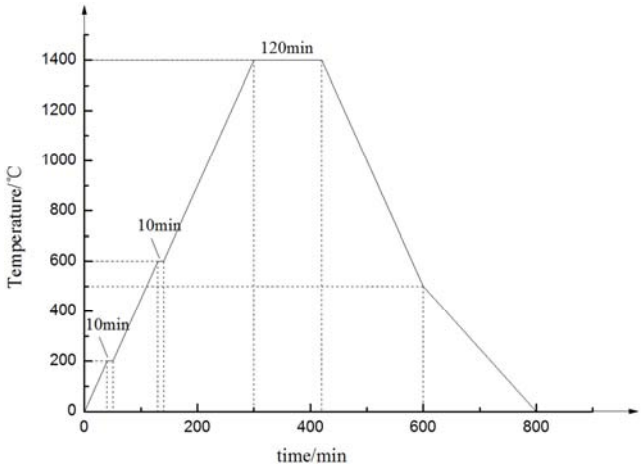

Figure 1. *Sintering regime for the samples.*

2.2. Equipment and Characterization

The crystal structures of the samples were confirmed by X-ray diffraction analysis (XRD, Rigaku D/max 2500v/pc) with Cu Kα radiation; The phase and plane index (*hkl*) were obtained by search/match using Jade 6.0. The surface morphologies of the gold-sprayed ceramic samples were observed using the SEM (JSM-6480 ESEM). The capacitance quantity (*C*) and dissipation factor (*D*) were measured with TZDM-200-300B testing system. The relative dielectric constant (ε_r) and dielectric loss ($tan\delta$) were calculated by the following Equations:

$$\varepsilon_r = \frac{14.4Ch}{\Phi^2} \quad (5)$$

$$\tan\delta = D \quad (6)$$

where *C* is the capacitance quantity (pF); *h* is the thickness (cm); Φ is the diameter of the electrode (cm); *D* is the dissipation factor. The temperature dependence of dielectric parameters was measured at 1~100 kHz from −150 to 150°C. The P-E hysteresis loops of Ho_2O_3 doped $(Ba_{0.75}Sr_{0.25})TiO_3$ ceramics at room temperature was obtained using the ferroelectric property test system.

3. Results and Discussion

3.1. XRD Analysis

The XRD patterns of Ho_2O_3 doped $(Ba_{0.75}Sr_{0.25})TiO_3$ ceramics are shown in Figure 2. It appears that all samples are single phase solid solutions with typical perovskite structure. No obvious secondary phase is found even for the 10 wt% Ho_2O_3 doped $(Ba_{0.75}Sr_{0.25})TiO_3$ ceramics based on the XRD patterns.

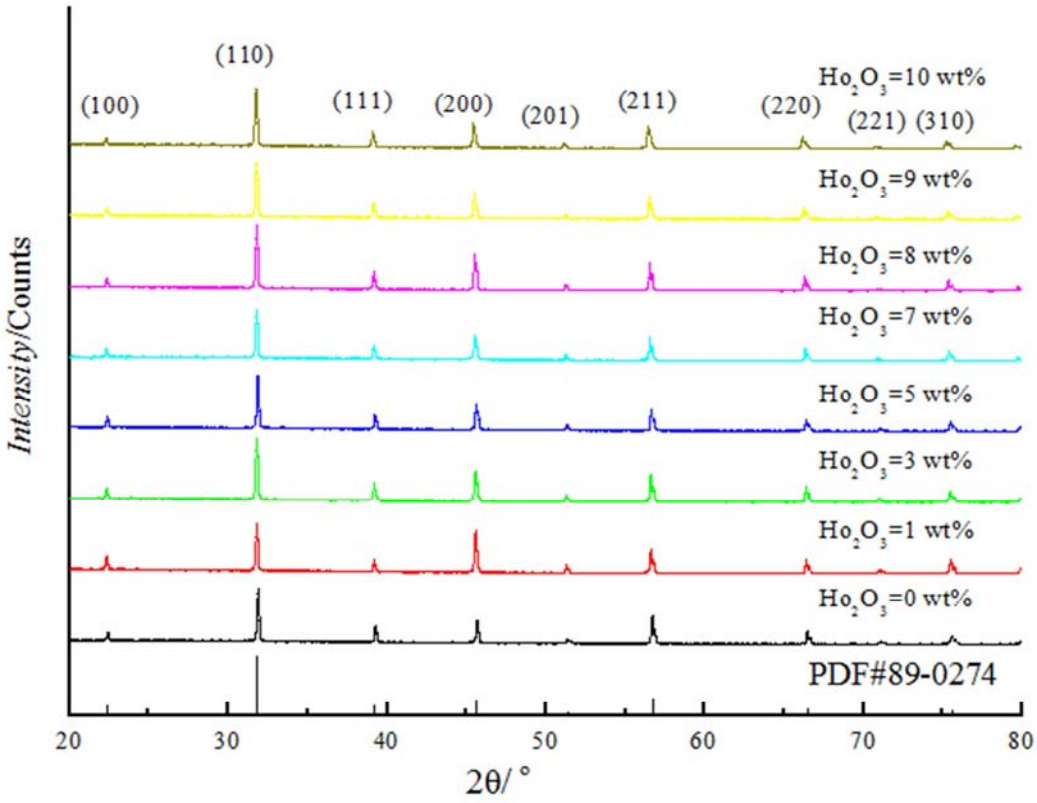

Figure 2. *XRD patterns of Ho_2O_3 doped $(Ba_{0.75}Sr_{0.25})$ TiO_3 ceramics.*

3.2. SEM Analysis

Figure 3 shows the SEM images of Ho_2O_3 doped $(Ba_{0.75}Sr_{0.25})$ TiO_3 ceramics. It appears that all samples exhibit dense microstructures and possess uniform grain size. With the increase of Ho_2O_3 doping content, the average grain size of $(Ba_{0.75}Sr_{0.25})$ TiO_3 ceramics decreases. The reason is that Ho^{3+} ions are easily segregated near the grain boundary, which hinders the further grain growth [17]. However, the cylindrical grains indicating the appearance of secondary phase (marked using red circles in Figure 3 (g) and (h)) which is not detected by XRD due to its small amount exist in the 9 and 10 wt% Ho_2O_3 doped $(Ba_{0.75}Sr_{0.25})$ TiO_3 ceramics.

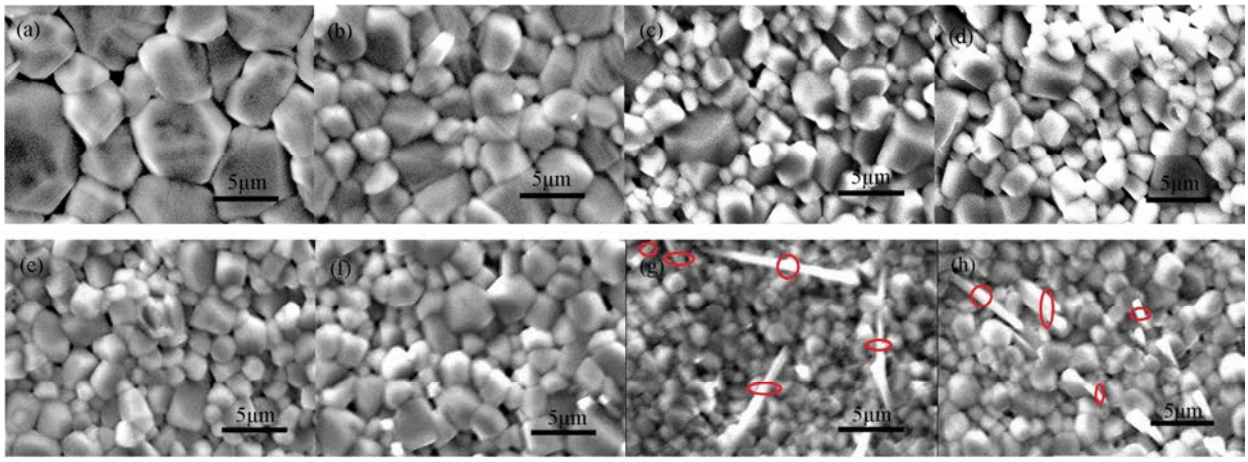

Figure 3. *SEM images of Ho_2O_3 doped $(Ba_{0.75}Sr_{0.25})$ TiO_3 ceramics: (a) Ho_2O_3=0 wt%; (b) Ho_2O_3=1 wt%; (c) Ho_2O_3=3 wt%; (d) Ho_2O_3=5 wt%; (e) Ho_2O_3=7 wt%; (f) Ho_2O_3=8 wt%; (g) Ho_2O_3=9 wt%; (h) Ho_2O_3=10 wt%.*

3.3. Dielectric Properties at Room Temperature

In the ABO_3 type perovskite structure, the coordination numbers of A and B site are 12 and 6, respectively. The radius of Ho^{3+} ion (1.23 Å, in 12 coordination) is smaller than that of Ba^{2+} ion (1.61 Å, in 12 coordination) and Sr^{2+} ion (1.44 Å, in 12 coordination); The radius of Ho^{3+} ion (0.90 Å, in 6 coordination) is bigger than that of Ti^{4+} ion (0.61 Å, in 6 coordination) [18]. Therefore, Ho^{3+} ion can substitute the A or B site of $(Ba_{0.75}Sr_{0.25})$ TiO_3 perovskite lattice. When Ho^{3+} ion

substitutes the A site, the point defect reaction is as follows:

$$2Ho_2O_3 + 4TiO_2 \rightarrow 4Ho_{Ba}^{\bullet} + 4Ti_{Ti} + 12O_O + O_2\uparrow + 4e' \quad (7)$$

When Ho^{3+} ion begins to substitute the B site, the point defect reaction can be expressed as follows:

$$2BaO + Ho_2O_3 \rightarrow 2Ba_{Ba} + 2Ho_{Ti}^{\bullet} + 5O_O + V_O^{\bullet\bullet} \quad (8)$$

Figure 4 shows the relative dielectric constant and dielectric loss of $(Ba_{0.75}Sr_{0.25})$ TiO_3 ceramics at room temperature with variation of Ho_2O_3 content. It is obvious that all ceramics possess high relative dielectric constant ($\varepsilon_r \geq 1.69\times10^3$) and low dielectric loss ($tan\delta \leq 6.4\times10^{-3}$) at room temperature. With the increase of Ho_2O_3 doping content, the relative dielectric constant of the system increases first and then decreases. The maximum of relative dielectric constant at room temperature can be found in the 1 wt% Ho_2O_3 doped $(Ba_{0.75}Sr_{0.25})$ TiO_3 ceramics. The dielectric loss of the system increases first, then decreases, and finally increases with the increase of Ho_2O_3 doping content.

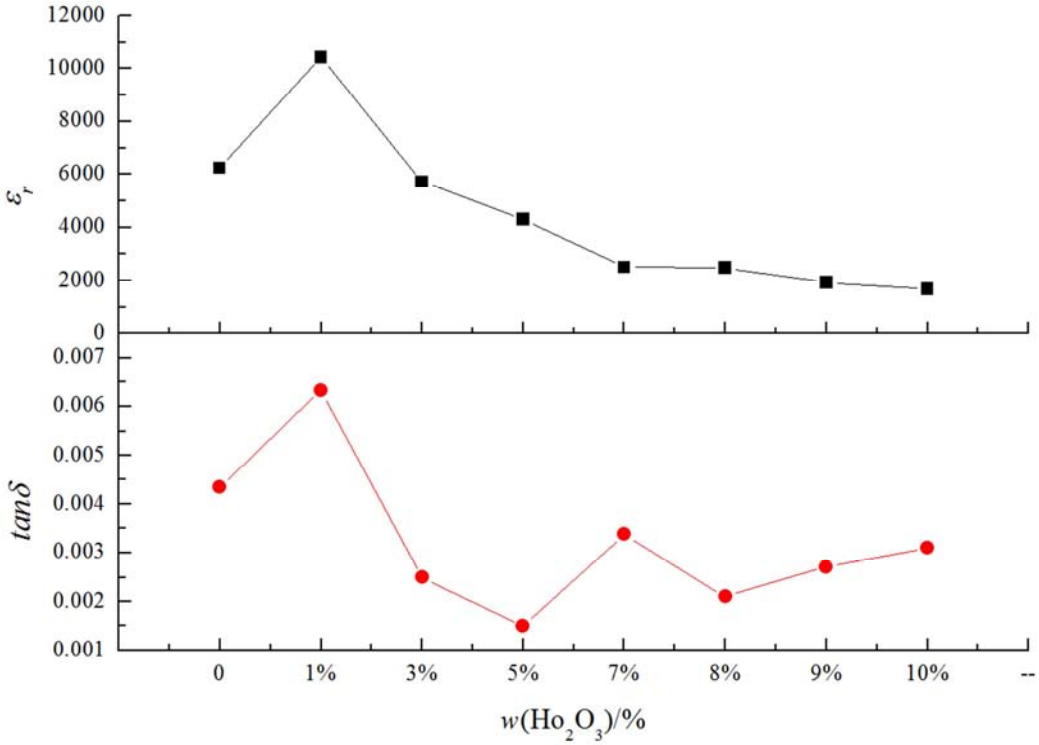

Figure 4. *ε_r and tanδ of Ho_2O_3 doped $(Ba_{0.75}Sr_{0.25})$ TiO_3 ceramics at room temperature.*

When $Ho_2O_3 \leq 1$ wt%, Ho^{3+} ions tend to substitute the A site ions of the perovskite lattice. The difference of the ionic radius causes the shrinkage deformation of the perovskite unit cells and the increase of the internal stress which result in the increase of relative dielectric constant [19]. When Ho_2O_3=1~8 wt%, Ho^{3+} ions gradually enter the B site. The bigger Ho^{3+} ions in the B site restrict the activity of B site ions and thus weaken the spontaneous polarization, which causes the relative dielectric constant decrease significantly with the increase of Ho_2O_3 doping content. When $Ho_2O_3 > 8$ wt%, non-ferroelectric secondary phase induced by the excessive Ho_2O_3 addition dilutes the ferroelectric phase, which makes the relative dielectric constant further decrease with the increase of Ho_2O_3 doping content [20].

As for the dielectric loss, When Ho^{3+} ions enter the A site of the perovskite lattice, the electrons as shown in Equation (7) are trapped by Ti^{4+} to form Ti^{3+}, leading to the increase of the dielectric loss gradually [21]. When Ho_2O_3=1~5 wt%, the weakened spontaneous polarization results in the decrease of the dielectric loss significantly with the increase of Ho_2O_3 doping content. On the other hand, the oxygen vacancies as shown in Equation (8) have pinning effect on the ferroelectric domains, which also causes the decrease of dielectric loss [22-24].

3.4. Temperature Dependence of the Relative Dielectric Constant and Dielectric Loss at Various Frequencies

Figure 5 shows the temperature dependence of the relative dielectric constant and dielectric loss at 1kHz~100kHz for Ho_2O_3 doped $(Ba_{0.75}Sr_{0.25})$ TiO_3 ceramics. When Ho_2O_3 content is higher than 5 wt%, the temperature corresponding to the maximum of relative dielectric constant (T_m) for $(Ba_{0.75}Sr_{0.25})$ TiO_3 ceramics shifts toward higher temperature obviously and the relative dielectric constant (in the $T<T_m$ range*)* decreases with the increase of test frequency, which is known as the frequency dispersion [25]. However, as indicated in Figure 5 (a)~(d), the $(Ba_{0.75}Sr_{0.25})$ TiO_3 ceramics with low Ho_2O_3 content do not exhibit permittivity frequency

dispersion. As shown in Figure 5 (c)~(h), the *tanδ* increases significantly with the increase of test frequency at low temperature; the *tanδ* is almost unaffected by the test frequency at high temperature, and the *tanδ* remains at a low value over a wide temperature range (room temperature~150°C), indicating that Ho_2O_3 doped $(Ba_{0.75}Sr_{0.25})TiO_3$ ceramics are promising for the application in capacitors as low dielectric loss dielectrics.

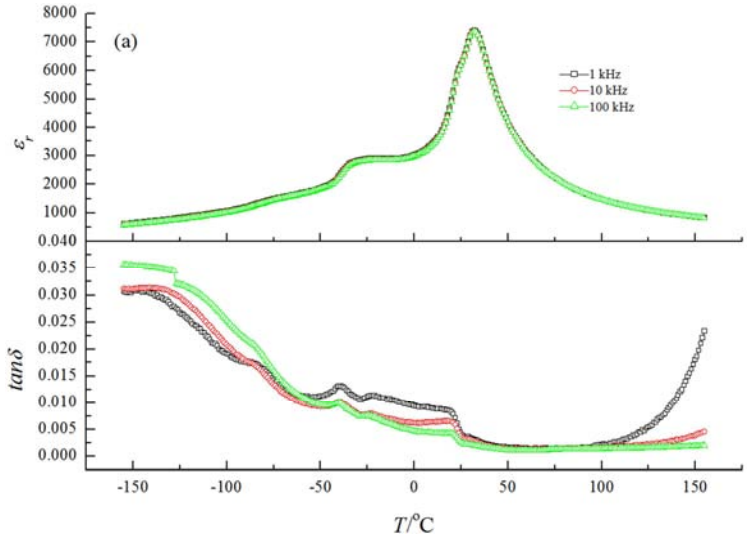

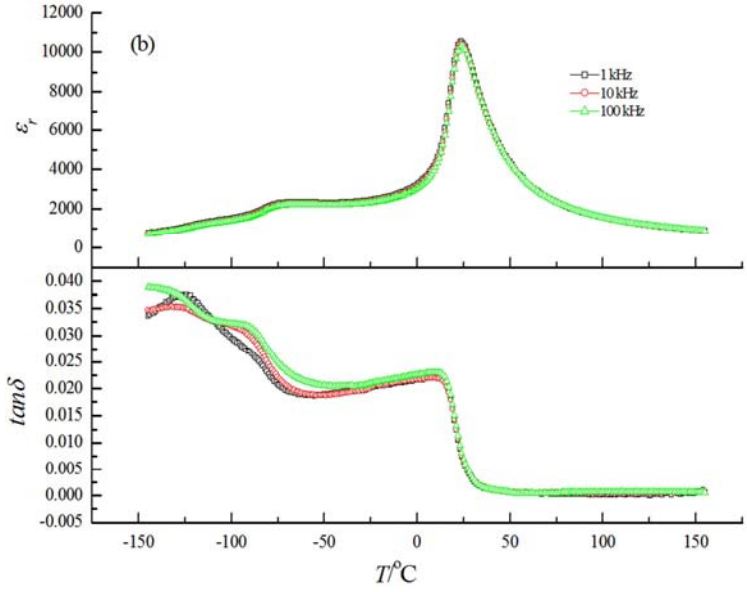

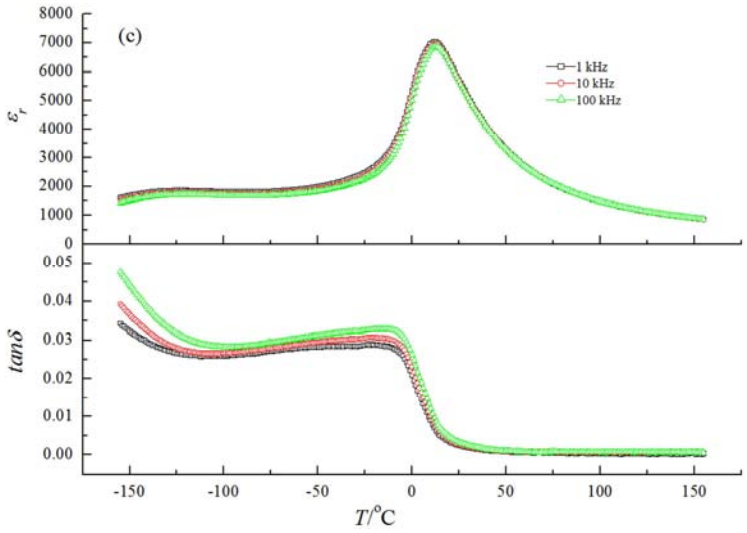

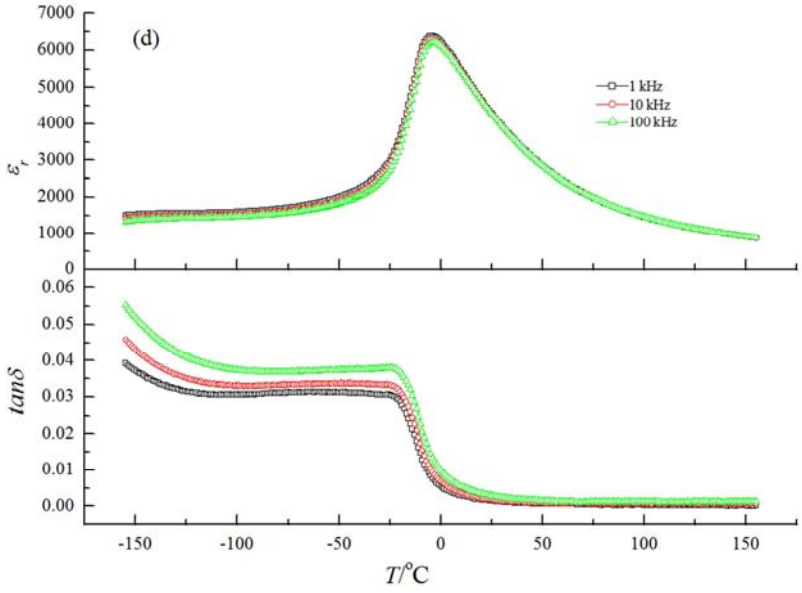
(d)
1 kHz
10 kHz
100 kHz
ε_r
tanδ
T/°C

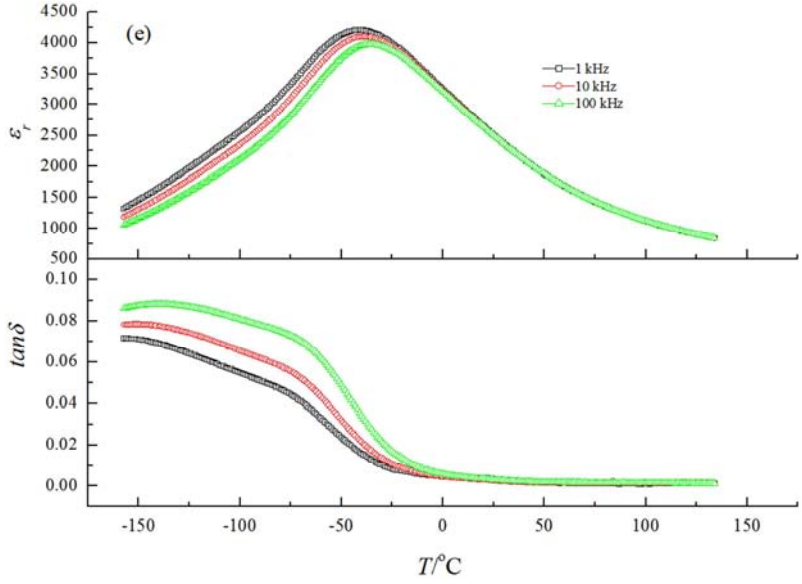
(e)
1 kHz
10 kHz
100 kHz
ε_r
tanδ
T/°C

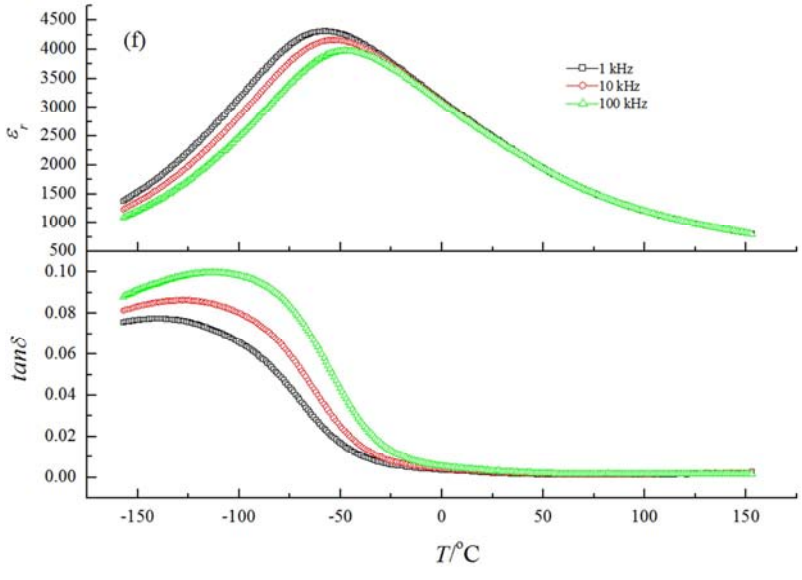
(f)
1 kHz
10 kHz
100 kHz
ε_r
tanδ
T/°C

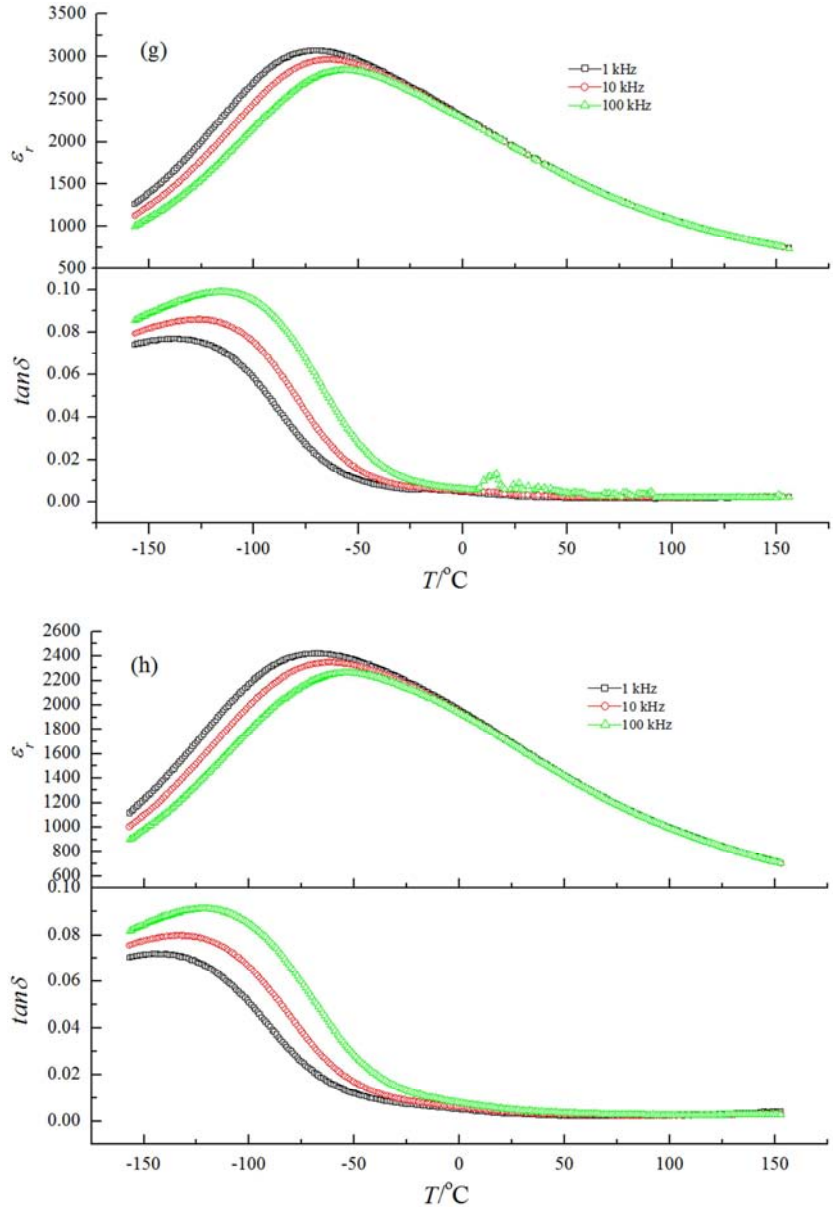

Figure 5. *Temperature dependence of the relative dielectric constant and dielectric loss of Ho_2O_3 doped $(Ba_{0.75}Sr_{0.25})$ TiO_3 ceramics: (a) Ho_2O_3=0 wt%; (b) Ho_2O_3=1 wt%; (c) Ho_2O_3=3 wt%; (d) Ho_2O_3=5 wt%; (e) Ho_2O_3=7 wt%; (f) Ho_2O_3=8 wt%; (g) Ho_2O_3=9 wt%; (h) Ho_2O_3=10 wt%.*

The maximum of relative dielectric constant (ε_{rmax}) and the temperature corresponding to this maximum (T_m) of $(Ba_{0.75}Sr_{0.25})$ TiO_3 ceramics with variation of Ho_2O_3 content are shown in Figure 6. When Ho_2O_3＞1 wt%, the T_m shifts toward lower temperature and the ε_{rmax} decreases with the increase of Ho_2O_3 doping content. The local deformation caused by Ho_2O_3 doping gives rise to the reduction of T_m. On the other hand, the non-ferroelectric layer in grain boundary of ferroelectric ceramics makes the ferroelectricity decrease, which causes T_m and ε_{rmax} decrease. As mentioned previously, the average grain size of Ho_2O_3 doped $(Ba_{0.75}Sr_{0.25})$ TiO_3 ceramics decreases with the increase of Ho_2O_3 doping content, which means that the grain boundary effect [26] is enhanced with the increase of Ho_2O_3 doping content and consequently makes the T_m and ε_{rmax} decrease.

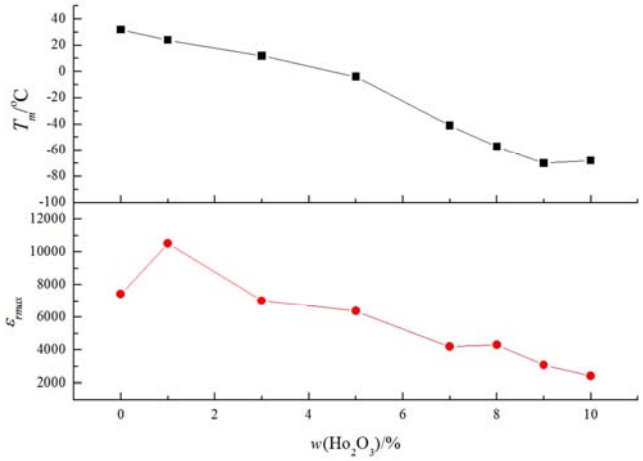

Figure 6. *T_m and ε_{rmax} of Ho_2O_3 doped $(Ba_{0.75}Sr_{0.25})$ TiO_3 ceramics.*

Since the diffuse phase transition is generally characterized by broadening in the dielectric constant (ε) versus temperature (T) curve, the full-width of half-maximum (FWHW) of ε_r-T curve is here calculated and listed in Table 1. It is notable that the FWHW increases from 31°C to 222.8°C when Ho_2O_3 content increases from 1wt% to 10wt%. In other words, the Curie peaks of high Ho_2O_3 concentration ceramics are more diffused and broadened than that of low Ho_2O_3 concentration ones. Since the typical diffuse phase transition and frequency dispersion of dielectric constant occurred in the $(Ba_{0.75}Sr_{0.25})$ TiO_3 ceramics with high Ho_2O_3 content, it can be concluded that with the increase of Ho_2O_3 doping content, $(Ba_{0.75}Sr_{0.25})$ TiO_3 ceramics are transformed into a relaxor-like ferroelectrics.

Table 1. *The FWHW of Ho_2O_3 doped $(Ba_{0.75}Sr_{0.25})$ TiO_3 ceramics.*

***W* (Ho_2O_3)/%**	**0**	**1**	**3**	**5**	**7**	**8**	**9**	**10**
FWHW/°C	41.1	31	56.1	65.9	159	166.9	197.8	222.8

3.5. Ferroelectric Properties

Figure 7 shows the *P*-*E* hysteresis loops of $(Ba_{0.75}Sr_{0.25})$ TiO_3 ceramics with different Ho_2O_3 doping content measured at room temperature. The typical *P*-*E* hysteresis loops can be found for undoped and 1 wt% Ho_2O_3 doped $(Ba_{0.75}Sr_{0.25})$ TiO_3 ceramics. Especially, compared with the undoped $(Ba_{0.75}Sr_{0.25})$ TiO_3 ceramics, the ferroelectricity of the 1 wt% Ho_2O_3 doped $(Ba_{0.75}Sr_{0.25})$ TiO_3 ceramics is enhanced, which exactly explains that the ε_{rmax} of the 1 wt% Ho_2O_3 doped $(Ba_{0.75}Sr_{0.25})$ TiO_3 ceramics achieve the maximum as shown in Figure 6. With the increase of Ho_2O_3 doping content, the *P*-*E* relationships turn out to be straight lines, implying the paraelectric phase for $(Ba_{0.75}Sr_{0.25})$ TiO_3 ceramics with high Ho_2O_3 content.

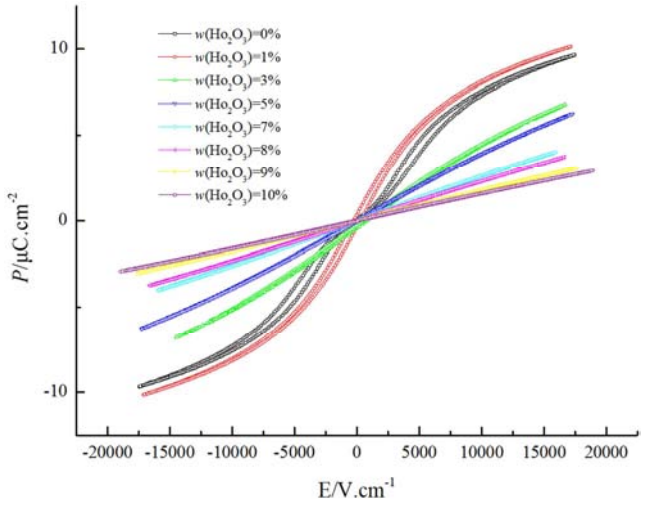

Figure 7. *P-E hysteresis loops of Ho_2O_3 doped $(Ba_{0.75}Sr_{0.25})$ TiO_3 ceramics.*

4. Conclusions

The Ho_2O_3 doped $(Ba_{0.75}Sr_{0.25})$ TiO_3 ceramics were prepared by solid state reaction method and their crystalline structure, surface morphology, dielectric and ferroelectric properties were investigated. The results show that:

(1) The proper Ho_2O_3 doping content is beneficial to obtaining fine grain structure. When Ho_2O_3>8 wt%, ceramic samples are multi-phase compounds with typical perovskite structure.

(2) Ho^{3+} ions enter the A and B site of perovskite lattice, causing lattice distortion of the system and affecting the relative dielectric constant and dielectric loss at room temperature. In addition, the electrons and oxygen vacancies produced in the substitution process also have a certain effect on the dielectric loss.

(3) The diffuse phase transition and frequency dispersion of dielectric constant reveal a relaxor characteristic of high Ho_2O_3 doped $(Ba_{0.75}Sr_{0.25})$ TiO_3 ceramics.

(4) According to the *P*-*E* hysteresis loops, the ferroelectricity is increased and then decreased with the increase of Ho_2O_3 doping content.

Acknowledgements

This work is supported by the Priority Academic Program Development of Jiangsu Higher Education Institutions and also sponsored by Suzhou Pant Piezoelectric Tech. Co. Ltd, China.

References

[1] A. Kaura, L. Singha, K. Asokan, Electrical relaxation and conduction mechanisms in iron doped barium strontium titanate, Ceramics International, (2007), doi: 10.1016/j.ceramint.2017.11.158.

[2] A. Kaur, A. Singh, L. Singh, S. K. Mishra, P. D. Babu, K. Asokan, S. Kumar, C. L. Chen, K. S. Yang, D. H. Wei, Structural, magnetic and electronic properties of iron doped barium strontium titanate, RSC Adv., 6 (2016) 112363–112369, doi: 10.1039/C6RA21458D.

[3] A. Ioachim, M. I. Toacsan, M. G. Banciu, L. Nedelcu, A. Dutu, S. Antohe, C. Berbecaru, L. Georgescu, G. Stoica, H. V. Alexandru, Transitions of barium strontium titanate ferroelectric ceramics for different strontium content, Thin solid Films, 515 (2007) 6289–6293, doi: 10.1016/j.tsf.2006.11.097.

[4] M. Paredes-Olguıín, I. A. Lira-Hernández, C. Gó mez-Yáñez, F. P. Espino-Cortés, Compensation mechanisms at high temperature in Y-doped $BaTiO_3$, Physica B, 410 (2013) 157-161, doi: 10.1016/j.physb.2012.11.001.

[5] Y. Tsur, A. Hitomi, I. Scrymgeour, C. A. Randall, Site occupancy of rare-earth cations in $BaTiO_3$, Japanese Journal of Applied Physics, 40 (2001), doi: 10.1143/jjap.40.255.

[6] D. Y. Lu, M. Sugano, M. Toda, High-permittivity double rare earth-doped barium titanate ceramics with diffuse phase transition, J. Am. Ceram. Soc., 89 (2006) 3112–3123, doi: 10.1111/j.1551-2916.2006.00893.x.

[7] D. Kim, J. Kim, T. Noh, J. Ryu, Y. N. Kim, H. Lee, Dielectric properties and temperature stability of $BaTiO_3$ co-doped La_2O_3 and Tm_2O_3, Curr. Appl. Phys., 12 (2012) 952–956, doi: 10.1016/j.cap.2011.12.016.

[8] L. Li, M. Wang, D. Guo, R. Fu, Q. Meng, Effect of Gd amphoteric substitution on structure and dielectric properties of $BaTiO_3$-based ceramics, J Electroceram, 30 (2013) 129-132, doi: 10.1007/s10832-012-9773-9.

[9] M. Borah, D. Mohanta, Effect of Gd^{3+} doping on structural, optical and frequency-dependent dielectric response properties of pseudo-cubic $BaTiO_3$ nanostructures, Appl. Phys. A, 115 (2014) 1057–1067, doi: 10.1007/s00339-013-7941-7.

[10] N. Masó, H. Beltrán, E. Cordoncillo, D. C. Sinclair, A. R. West, Polymorphism and dielectric properties of Nb-doped $BaTiO_3$. J. Am. Ceram. Soc., 91 (2008) 144-150, doi: 10.1111/j.1551-2916.2007.02083.x.

[11] F. D. Morrison, A. M. Coats, D. C. Sinclair, A. R. West, Charge compensation mechanisms in La doped $BaTiO_3$, Journal of Electroceramics, 6 (2001) 219-232, doi: 10.1023/a:1011400630449.

[12] D. Y. Lu, Study on the modification of barium titanate ceramic structure by lanthanide ions in the field of dielectric, Journal of jilin institute of chemical technology, 25 (2008) 34-41, doi: 10.16039/j.cnki.cn22-1249.2008.01.006.

[13] Y. L. Li, Y. F. Qu, Dielectric properties and substitution mechanism of samarium-doped $Ba_{0.68}Sr_{0.32}TiO_3$ ceramics, Materials Research Bulletin, 44 (2009) 82-85, doi: 10.1016/j.materresbull.2008.03.030.

[14] C. Zhao, X. Y. Huang, H. Guan, C. H. Gao, Effect of Y_2O_3 and Dy_2O_3 on dielectric properties of $Ba_{0.7}Sr_{0.3}TiO_3$ series capacitor ceramics, Journal of Rare Earths, 25 (2007) 197-200, doi: 10.1016/S1002-0721 (07) 60468-2.

[15] W. Yang, A. M. Chang, B. C. Yang, Effect of grain size on dielectric and ferroelectric Properties of $Ba_{0.80}Sr_{0.20}TiO_3$ ceramics, Journal of the Chinese Ceramic Society, 3 (2002) 390-397, doi: 10.3321/j.issn:0454-5648.2002.03.024.

[16] Z. Li, P. Zhao, X. H. Xue, Z. T. Li, Z. Wang, L. Xu，H. Q. Fan, Structure and Electrical Properties of $Ba_{l-x}Sr_xTiO_3$ Ceramics with Various Sintering Processes, Materials Review, 30 (2016) 55-59, doi: 10.11896/j.issn.1005-023X.2016.16.012.

[17] Y. P. Pu, S. F. Ning, W. Chen, Influence of Dy_2O_3 doping on the structure and properties of $BaTiO_3$ ceramics, Journal of Xi'an Jiao Tong University, 38 (2004) 424-427, doi: 10.3321/j.issn:0253-987X.2004.04.024.

[18] F. Zhou, G. F. Liu, J. B. Wang, J. Li, X. B. Cao, Influence of doping on dielectric properties of barium strontium titanate ceramics, Insulating material, 42 (2009) 46-48, doi: 10.16790/j.cnki.1009-9239.im.2009.03.011.

[19] C. Zhang, Y. F. Qu, Dielectric properties and phase transitions of La_2O_3 and Sb_2O_3 doped barium strontium titanate ceramics, Trans. Nonferrous Met. Soc. China, 22 (2012) 2742-2748, doi: 10.1016/S1003-6326 (11) 61527-6.

[20] X. Y. Huang, R. K. XING, S. J. Guo, Influence of Nd_2O_3 content on the low temperature sintering of BST ceramic. Electronic Components and Materials, 33 (2014) 10-16, doi: 10.14106/j.cnki.1001-2028.2014.12.003.

[21] W. Li, J. Qi, Y. Wang, L. Li, Z. Gui, Doping behaviors of Nb_2O_5 and Co_2O_3 in temperature stable $BaTiO_3$ ceramics, Materials Letters, 57 (2002) 1-5, doi: 10.1016/S0167-577X (02) 00687-0.

[22] B. Su, T. W. Button, Microstructure and dielectric properties of Mg-doped barium strontium titanate ceramics, Journal of Applied Physics, 95 (2004) 1382-1385, doi: 10.1063/1.1636263.

[23] Y. Li, R. Wang, X. Ma, Z. Li, R. Sang, Y. Qu, Dielectric behavior of samarium doped $BaZr_{0.2}Ti_{0.8}O_3$ ceramics, Materials Research Bulletin, 49 (2014) 601-607, doi: 10.1016/j.materresbull.2013.10.001.

[24] C. Zhang, Z. X. Ling, G. Jian, F. X. Chen, Dielectric properties and point defect behavior of antimony oxide doped Ti deficient barium strontium titanate ceramics, Trans. Nonferrous Met. Soc. China, 27 (2017) 2656-2662, doi: 10.1016/S1003-6326 (17) 60294-2.

[25] K. Wang, A. Hussain, W. Jo, J. Rodel, Temperature-dependent properties of $(Bi_{1/2}Na_{1/2})$ TiO_3- $(Bi_{1/2}K_{1/2})$ TiO_3- $SrTiO_3$ lead-free piezoceramics, J. Am. Ceram. Soc., 95 (2012) 2241-2247, doi: 10.1111/j.1551-2916.2012.05162.x.

[26] C. Zhang, Z. X. Ling, G. Jian, The defect chemistry and dielectric properties of Sb_2O_3 doped non- stoichiometric barium strontium titanate ceramics, J Mater Sci: Mater Electron, 27 (2016) 11770-11776, doi: 10.1007/s10854-016-5316-5.